Pathology - Research and Practice 215 (2019) 152677

Contents lists available at ScienceDirect

Pathology - Research and Practice

journal homepage: www.elsevier.com/locate/prp

Sanguinarine inhibits the tumorigenesis of gastric cancer by regulating the TOX/DNA-PKcs/ KU70/80 pathway

Hui-Ning Fan, Wei Chen, Shi-Qiao Peng, Xiao-Yu Chen, Rui Zhang, Rui Liang, Hui Liu, Jin-Shui Zhu*, Jing Zhang*

Department of Gastroenterology, Shanghai Jiao Tong University Affiliated Sixth People's Hospital, Shanghai, 200233, China

ARTICLE INFO

Keywords:
Sanguinarine
Gastric cancer
TOX
DNA-PKcs
KU70
KU80

ABSTRACT

Sanguinarine (SAG), a benzophenanthridine alkaloid extracted from *Sanguinaria canadensis*, exerts antioxidant, anti-inflammatory and antiproliferative activities in a variety of malignancies. However, the underlying mechanisms by which SAG affects the tumorigenesis of gastric cancer (GC) are unclear. The common targets of SAG and GC were identified by network pharmacology, and the association of thymocyte selection-associated high mobility group box (TOX) with the clinicopathological characteristics and prognosis of patients with GC was analyzed by using datasets from The Cancer Genome Atlas (TCGA). 3-(4,5-Dimethyl-2-thiazolyl)-2,5-diphenyl-2-H-tetrazolium bromide (MTT) assays, colony formation assays, flow cytometry analysis, and a xenograft tumor model were conducted to assess the effects of SAG on the growth of GC cells, and Quantitative real-time polymerase chain reaction (qRT-PCR) and Western blot analysis were used to determine the effects of SAG on the TOX/DNA-PKcs/KU70/80 signaling pathway. We identified 9 collective targets of SAG and GC, of which TOX expression levels were dramatically downregulated in GC tissues compared with adjacent normal tissues, and a low expression of TOX served as an independent prognostic factor of poor survival in patients with GC. SAG suppressed cell viability, colony formation and *in vivo* tumorigenesis and induced cell apoptosis and cell cycle arrest. Furthermore, SAG increased the expression levels of TOX but decreased those of DNA-PKcs and KU70/80 in GC cells. Our findings indicate that SAG inhibits the tumorigenesis of GC cells by regulating TOX/DNA-PKcs/KU70/80 signaling and may provide therapeutic strategies for the treatment of GC.

1. Introduction

Gastric cancer (GC) is a malignant disease of the digestive tract with high incidence and mortality. Despite the application of digestive endoscopy in the diagnosis and treatment of GC, the prognosis of the patients remains relatively poor, with a 5-year survival rate of less than 40% due to tumor recurrence and metastasis [1]. GC is characterized by genome instability through DNA damage caused by various factors [2], of which the catalytic subunits of DNA-dependent protein kinase (DNA-PKcs) bind with the KU70/80 heterodimer to form DNA-dependent protein kinase (DNA-PK), a key promoter of the nonhomologous end joining (NHEJ) pathway [3,4]. Accumulating evidence shows that the dysregulation of DNA-PKcs/KU70/80 signaling is associated with the pathological processes of various malignancies [5,6].

Thymocyte selection-associated high mobility group box (TOX), a member of an evolutionarily conserved DNA-binding protein, participates in regulating cell apoptosis, growth, metastasis, and DNA repair [7]. The aberrant expression of TOX is associated with tumor progression by regulating $CD4^+$ T-cell and *Fusobacterium nucleatum* infection [8–13] and determines tumor growth by binding with KU70/80 and inhibiting NHEJ repair [12].

Sanguinarine (SAG), a benzophenanthridine alkaloid, is regarded as a 'secondary metabolite' or 'natural product' in plants [14]. It was initially used for the treatment of dental diseases owing to its repressive nature against fungi, bacteria and inflammation [15]. Recent studies have shown that SAG possesses antitumor potential by inducing cell apoptosis and repressing proliferation, angiogenesis and invasion [16,17], but the underlying mechanisms of SAG in GC remain unknown. In the present study, we first identified the common targets of SAG and GC and confirmed that the decreased expression of TOX was associated with poor survival in patients with GC. Moreover, SAG inhibited the tumorigenesis of GC by regulating TOX/DNA-PKcs/KU70/80 signaling and might provide a therapeutic strategy for the treatment of GC.

* Corresponding authors at: Department of Gastroenterology, Shanghai Jiao Tong University Affiliated Shanghai Sixth People's Hospital, No. 600 Yishan Road, Shanghai 200233, China.

E-mail addresses: zhujs1803@163.com (J.-S. Zhu), jing5522724@163.com (J. Zhang).

https://doi.org/10.1016/j.prp.2019.152677
Received 12 August 2019; Received in revised form 17 September 2019; Accepted 27 September 2019

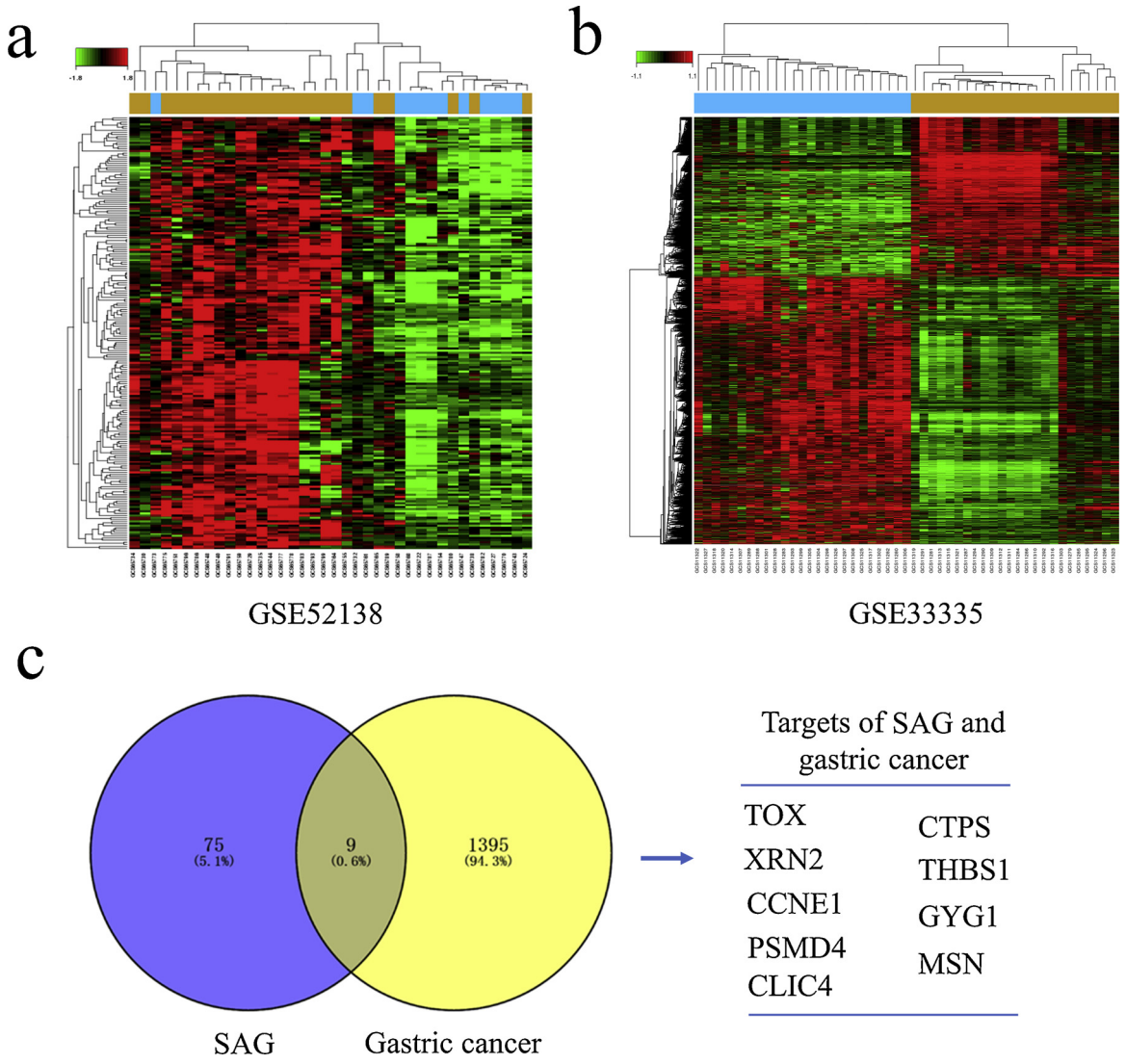

Fig. 1. Identification of the common targets of SAG and GC. (a, b) The differentially expressed genes were screened between GC and adjacent normal tissues from the GSE52138 and GSE33335 datasets. (c) Nine collective targets of SAG and GC were obtained by using the Venn diagram.

2. Materials and methods

2.1. Reagents and compounds

SAG (purity ≥98%) was purchased from Dalian Meilun Biotechnology Co., Ltd. (Dalian, China). 3-(4,5-Dimethyl-2-thiazolyl)-2,5-diphenyl-2-H-tetrazolium bromide (MTT) was purchased from Shanghai Beyotime Biotechnology Co., Ltd. (Shanghai, China). All the supplies for cell culture were purchased from Thermo Fisher Scientific Company (Waltham, MA, USA). The GC cell lines (SGC-7901 and AGS) and GES-1 used in these experiments were from the Laboratory of Gastroenterology of our Hospital. Lentivirus-mediated TOX over-expression vectors, negative control vectors (NC) and virion-packaging elements were purchased from Genechem (Shanghai, China).

2.2. Clinical samples

The clinicopathological data of 32 paired GC and 415 unpaired GC tissue samples as well as the expression levels of 9 targets (TOX, XRN2, CCNE1, PSMD4, CLIC4, CTPS, THBS1, GYG1 and MSN) were downloaded from The Cancer Genome Atlas (TCGA) RNA-seq database (https://genome-cancer.ucsc.edu). The protocols used in our study were approved by the Ethics Committee of the Shanghai Sixth People's Hospital.

2.3. Identification of the common targets of SAG and GC

The canonical simplified molecular-input line-entry system (SMILES) of SAG {C[N+]1=C2C(=C3C = CC4=C(C3 = C1)OCO4)C = CC5=CC6=C (C = C52)OCO6} was acquired by Pubchem (https://pubchem.ncbi.nlm.nih.gov/) and was used to screen the targets of SAG by using SwissTargetPrediction (http://www.swisstargetprediction.ch/) and PharmMapper. The targets of GC were identified by using Gene-Cloud of Biotechnology Information (GCBI) and Gene Expression Omnibus (GEO) datasets (https://www.gcbi.com.cn/gclib/html/index). The common targets of SAG and GC were obtained by Venny 2.1 (http://bioinfogp.cnb.csic.es/tools/venny/index.html).

2.4. Cell culture and cell transfection

GC cells (SGC-7901 and AGS) and GES-1 were cultured in DMEM containing 10% fetal bovine serum (FBS), penicillin (100 U/ml) and streptomycin (100 g/ml) and incubated at 37 °C, 5% CO2 and saturated humidity. Lentivirus vectors for transfection were prepared and transfected into SGC-7901 and AGS cells.

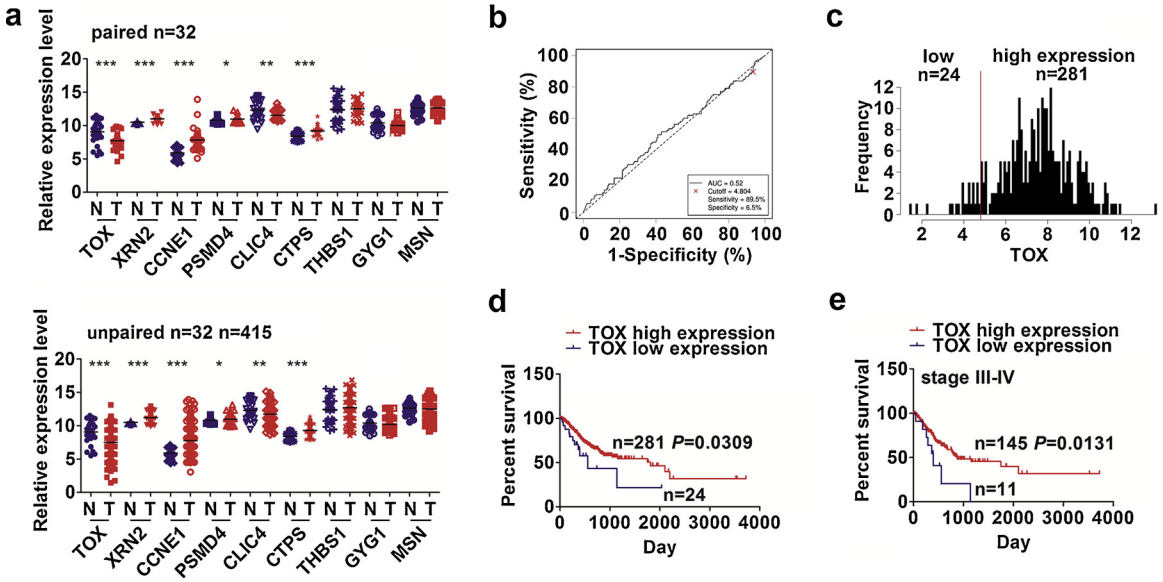

Fig. 2. The association of TOX expression with overall survival in patients with GC. (a) TCGA analysis of the expression levels of 9 target genes in paired and unpaired GC tissues. (b) ROC curve analysis of the cutoff value of TOX in GC patients. (c) The cutoff value of TOX divided the patients into high TOX expression and low TOX expression groups. (d, e) Kaplan-Meier analysis of the association of TOX expression with survival in GC patients and late-stage patients. * $P < 0.05$, ** $P < 0.01$, *** $P < 0.001$.

2.5. MTT assay

GC cells (2×10^3 μl/well) were seeded in 96-well plates and incubated for 24 h at 5% CO2 and saturated humidity. Then, serial concentrations of SAG (0, 1.25, 2.5, and 5 μM) were added to each well. After treatment for 24, 48, and 72 h, MTT (10 μl) was added into each well, followed by incubation for 1 h. The optical density (OD) at 490 nm was measured using a microplate reader (Molecular Device, Sunnyvale, CA, USA).

2.6. Colony formation assays

Briefly, GC cells (1×10^4) were plated into 10 cm dishes and cultured for 15 days. Colonies were then fixed with methanol for 15 min and stained with 0.1% crystal violet for 10 ~30 min. The number of colonies containing > 10 cells was counted under a microscope. Experiments were performed three times.

2.7. Flow cytometry analysis

GC cells were collected after incubation with different concentrations of SAG (0, 1.25, 2.5, and 5 μM) for 24 h, and then, the cells were blocked in 70% ethanol at 4 °C overnight. The cells were centrifuged (1000 rpm for 5 min) and then washed with phosphate-buffered saline (PBS), followed by staining with propidium iodide (PI, 1 ml). Then, the cell cycle distribution was analyzed by an FC 500 flow cytometer (Beckman, Brea, CA, USA). Apoptosis analyses were conducted by the Annexin V-FITC Apoptosis Detection Kits (Beyotime, Shanghai, China) following the manufacturer's instructions.

2.8. qRT-PCR

Total RNA was extracted from the cultured cells of the experimental groups using TRIzol reagent (Invitrogen, Katlsruhe, Germany) according to the manufacturer's instructions and was then reversely transcribed to cDNA by using a first-strand cDNA synthesis kit (Takara, Dalian, China). Quantitative real-time polymerase chain reaction (qRT-PCR) was performed by an ABI 7500 PCR instrument (Applied Biosystems, Shanghai, China) using a SYBR green PCR kit (TaKaRa, Dalian, China). The amplification reaction conditions were as follows: 95 °C for 30 s, 60 °C for 30 s and 72 °C for 60 s. This procedure was repeated for 30 cycles. The relative mRNA expression was calculated by the comparative Ct ($2^{-\Delta\Delta Ct}$) method. Glyceraldehyde-3-phosphate dehydrogenase (GAPDH) was always tested as the reference gene. The primers of TOX and GAPDH were designed and synthesized by Shanghai Genechem Co., Ltd (Shanghai, China). The primer sequences were as follows: TOX, F: 5'CGGGAATGAATCCTCACCTAAC3′ and R: 5' CAGTCACTGGCATTTGGTTATTC3′; and GAPDH, F: 5'GCACCGTCAAG GCTGAGAAC3′ and R: 5'TGGTGAAGACGCCAGTGGA3′.

2.9. Western blot analysis

The protein abundance in the cells was determined by Western blot analysis. Cells (5×10^6) in the logarithmic growth phase were collected and lysed for total proteins. The supernatant fluid of the lysates was collected by centrifugation (12,000 rpm for 10 min), followed by SDS-PAGE. After electrophoresis, the proteins were electrotransferred onto a polyvinylidene fluoride (PVDF; Millipore Boston, MA, USA) membrane. The membrane was then rinsed with a blocking solution of 5% nonfat milk for 60 min and incubated overnight at 4 °C with antibodies against TOX (bs-17327R, Bioss, Shanghai, China), DNA-PKcs (AF1888, Beyotime, Shanghai, China), KU70 (AF0213, Beyotime, Shanghai, China) and KU80 (AF1981, Beyotime, Shanghai, China), followed by incubation with secondary antibodies at room temperature for 1 h. Enhanced chemiluminescence (ECL) reagents (Boster, Shanghai, China) were used to visualize the targeted protein bank under X-ray film. GAPDH was used as a control.

2.10. Xenograft tumor models

For the xenograft tumor model in nude mice, 1×10^6 SGC-7901 cells were suspended in 200 μl of sterile PBS and injected subcutaneously into the right flank of male BALB/C nude mice (4–6 weeks). When tumors reached an average size of 50 mm^3, the mice were randomized into three groups: control group (saline, n = 6), low-dose SAG group (4 mg/kg, n = 6) and high-dose SAG group (8 mg/kg, n = 6); saline or SAG was administered every day for 3 weeks. The body weight of the mice and the two perpendicular diameters (length

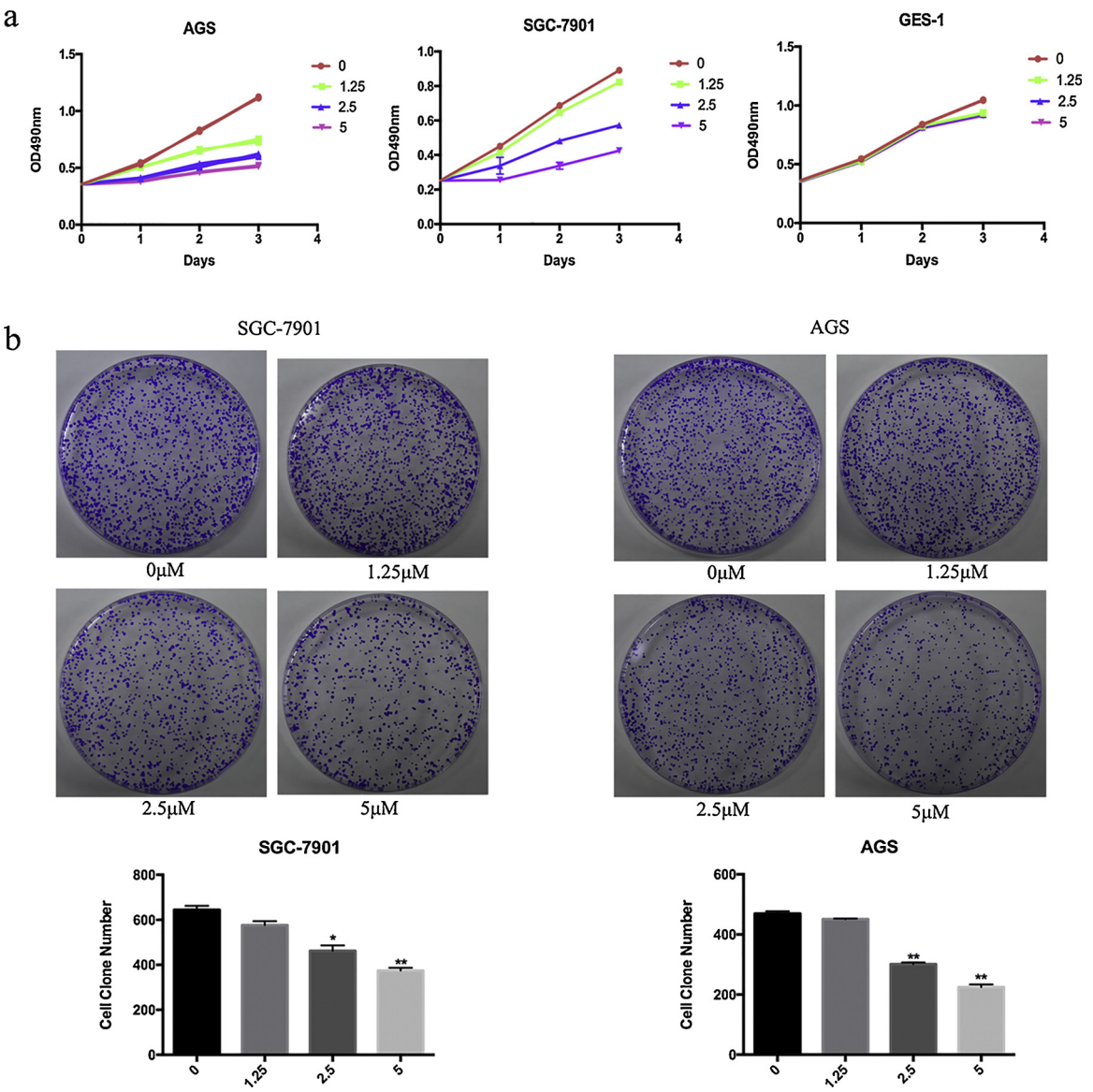

Fig. 3. SAG inhibited the proliferation and colony formation of GC cells. (a) MTT and (b) colony formation assays were performed to assess the effects of SAG on the proliferation and cell colony numbers in SGC-7901 and AGS cells in a dose- and time-dependent manner. Data are the means ± SEM of three experiments. * $P < 0.05$, ** $P < 0.01$.

and width) of the tumors were recorded, and tumor size was calculated according to the following formula: volume (V) = (LW^2)/2, where 'L' represents the largest length and 'W' represents the smallest width. At 21 days post intragastric tumor formation, the mice were euthanized, and the tumors were excised, paraffin-embedded, and formalin-fixed. Hematoxylin and eosin (H&E) staining and immunostaining analysis were performed. All animal work was approved by the Animal Care Committee of our Hospital.

2.11. Immunohistochemistry (IHC) analysis

IHC analysis was performed to examine the protein expression levels, including those of Ki-67, TOX, DNA-PKcs, and KU70. Briefly, the tumor tissue slides, which were deparaffinized, rehydrated, and antigen-retrieved with 10 mM sodium citrate buffer (pH 6.0, at 90 °C for 30 min), were blocked and antibody-incubated. The slides were pre-incubated with 0.04% bovine serum albumin to block nonspecific binding. Subsequently, the slides were incubated with primary polyclonal antibodies (ABclonal Biotech, Shanghai, China) at a dilution of 1:200 overnight at 4 °C and then with secondary antibodies (KeyGen Biotech, Shanghai, China) at room temperature for 1 h. Finally, the sections were stained with 3,3-diaminobenzidine (DAB) and counterstained with hematoxylin. Images were visualized under a microscope (Olympus, Tokyo, Japan).

2.12. Statistical analysis

Data are expressed as the mean ± standard deviation (SD). Analysis of variance (ANOVA) and Student's *t*-test were used to determine significant differences. The Kaplan-Meier method was used to determine the association of the target genes with poor prognosis in patients with GC. Experimental data were assessed with GraphPad Prism 7 (La Jolla, CA, USA). *P* values of less than 0.05 were considered significant.

3. Results

3.1. Identification of the common targets of SAG and GC

As indicated in Supplementary Table S1, approximately 75 target

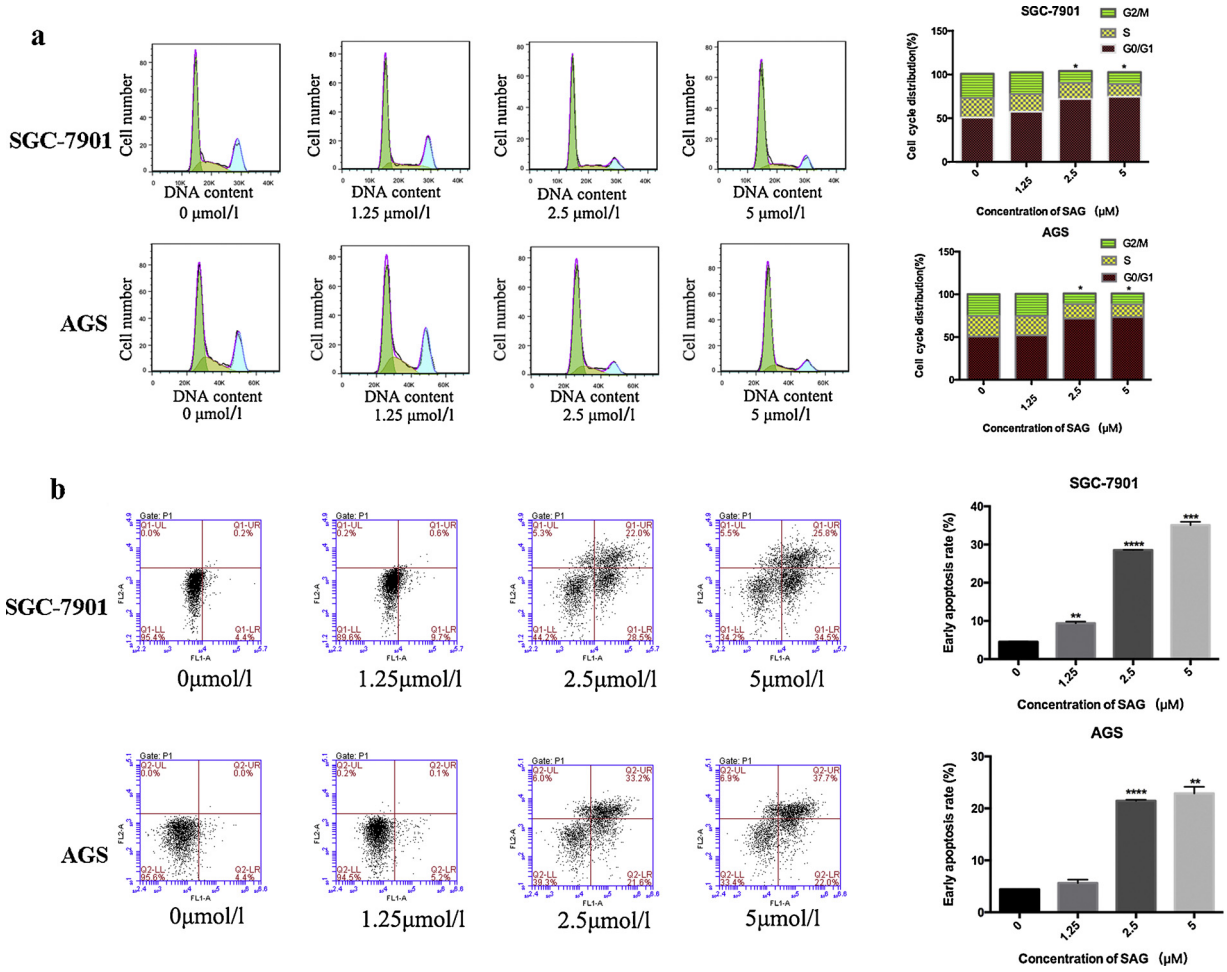

Fig. 4. SAG induced cell cycle arrest and apoptosis in GC cells. (a, b) Flow cytometry analysis was conducted to estimate the effects of SAG on the cycle distribution and cell apoptotic index of SGC-7901 and AGS cells in a dose- and time-dependent manner. Data are the means ± SEM of three experiments. * $P < 0.05$, ** $P < 0.01$, *** $P < 0.001$, **** $P < 0.0001$.

genes of SAG were identified by using network pharmacology, and 1395 target genes of GC were acquired from the public database GEO, of which 395 differentially expressed genes between GC and adjacent normal tissues were from GSE52138 (Fig. 1a and Supplementary Table S2), and another 1000 were from GSE33335 (Fig. 1b and Supplementary Table S3). Thus, 9 collective targets of SAG and GC were obtained by using a Venn diagram (Fig. 1c).

3.2. Low expression of TOX was associated with poor survival in patients with GC

We analyzed the expression levels of these 9 targets in GC tissues and found that TOX ($P < 0.001$), XRN2 ($P < 0.001$), CCNE1 ($P < 0.001$) and CTPS ($P < 0.001$) were the most significantly differentially expressed between GC and normal tissues, of which TOX expression levels were decreased, but XRN2, CCNE1and CTPS levels were increased in paired and unpaired GC tissues (Fig. 2a). According to the gene expression levels, survival time and survival status, cutoff values for TOX, XRN2, CCNE1 and CTPS were determined in GC patients (Fig. 2b and Supplementary Figure S1) and were used to divide the patients into high expression and low expression groups (Fig. 2c and Supplementary Figure S1).

Then, we analyzed the association of these four genes with the prognosis of patients with GC and found that a low expression of TOX had no association with the clinicopathological characteristics in patients with GC (Supplementary Table S4). These patients and those in the late stage (stage III + IV) with low TOX expression exhibited a poorer survival than those with high TOX expression (Fig. 2d, e), but there was no difference in tumor recurrence, and those in the early stage (stage I + II) also showed no difference in overall survival (Supplementary Figure S2). Univariate and multivariate analyses revealed that low TOX expression and age were independent prognostic factors of poor survival in patients with GC (Supplementary Table S5). However, the increased expression of XRN2, CCNE1 and CTPS displayed a contradictory trend with a longer survival or lower recurrence in GC patients (Supplementary Figure S1). Therefore, TOX was selected for further analysis.

3.3. SAG inhibited the cell proliferation and colony formation of GC cells

The viability of GC cells (SGC-7901 and AGS) was detected after exposure to different concentrations of SAG at different time points. The results indicated that SAG produced marked inhibitory effects on the cell proliferation and colony formation of SGC-7901 and AGS cells in a dose- and time-dependent manner but exerted no impact on those of GES-1 cells compared with the control group (Fig. 3a, b).

3.4. SAG induced cycle arrest and the apoptosis of GC cells

Flow cytometry analysis was used to determine the cell cycle distribution and cell apoptosis after exposure to different concentrations of SAG at different time points. The results indicated that compared with

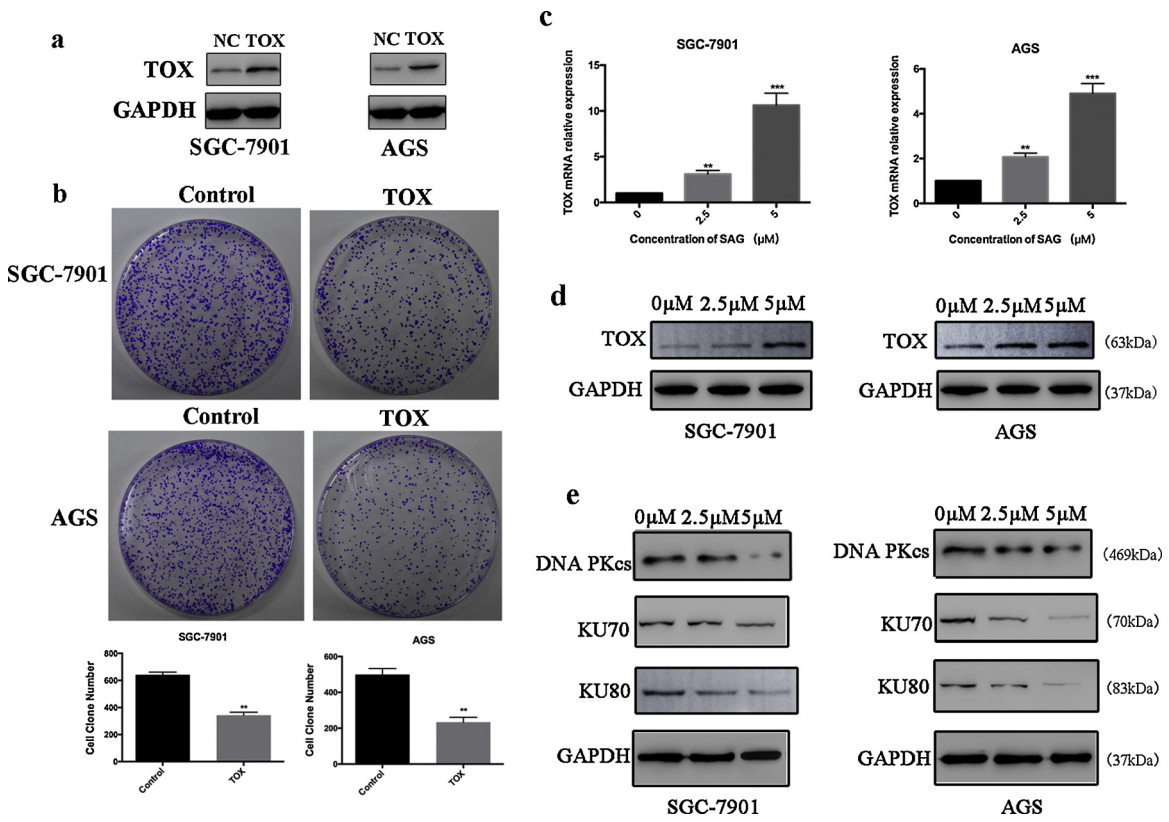

Fig. 5. TOX inhibited GC cell proliferation and the effects of SAG on the expression of TOX/DNA-PKcs/KU70/80 in GC cells. (a) TOX protein expression was examined by Western blot analysis in TOX-transfected SGC-7901 and AGS cells. (b) Clone formation assays indicated that the overexpression of TOX inhibited GC cell proliferation after TOX transfection. (c) qRT-PCR and (d) Western blot analysis of the effects of SAG on TOX expression levels in SGC-7901 and AGS cells. (e) Western blot analysis of the effects of SAG on the expression of DNA-PKcs and KU70/80 in SGC-7901 and AGS cells. Data are the means ± SEM of three experiments. * $P < 0.05$, ** $P < 0.01$, *** $P < 0.001$.

the control group, SAG treatment (2.5 and 5 μM for 24 h) increased the proportion of GC cells in the G0/G1 phase and decreased the proportion of GC cells in the S phase (Fig. 4a). Then, Annexin V/PI double staining was performed to assess cell apoptosis, and the results indicated that SAG induced dramatically increased cell apoptosis in a dose-dependent manner compared with that in the control group (Fig. 4b).

3.5. TOX overexpression inhibited GC cell proliferation, and SAG regulated the expression of TOX/DNA-PKcs/KU70/80 in GC cells

To confirm the function of TOX in GC cells, TOX was stably overexpressed through a lentiviral vector in SGC-7901 and AGS cell lines, and was determined by Western blot analysis (Fig. 5a). To verify the role of TOX in GC growth, cell proliferation was determined by clone formation. The results demonstrated that the overexpression of TOX significantly decreased cell proliferation in GC cells compared with that of the control group ($P < 0.01$). After exposure to different concentrations of SAG for 24 h, qRT-PCR and Western blot analysis were conducted to measure the expression levels of TOX/DNA-PKcs/KU70/80 in SGC-7901 and AGS cells. The results indicated that SAG substantially elevated the expression levels of TOX (Fig. 5c, d) but significantly reduced those of downstream DNA-PKcs and KU70/80 in SGC-7901 and AGS cells in a dose-dependent manner compared with those of the control group (Fig. 5e).

3.6. SAG inhibited the xenograft tumor growth

Given that SAG exerted anti-GC effects *in vitro*, the potential effects of SAG on GC cell growth *in vivo* were further investigated by establishing a xenograft tumor model, which showed that the mice with the gavage administration of low- or high-dose SAG displayed a lower tumor volume and weight than those of the control group (Fig. 6a). H&E staining demonstrated that the tumor formation ability was lowered by the administration of SAG compared with that of the control group (Fig. 6b) IHC analysis showed that SAG significantly reduced the expression levels of Ki-67, KU70, and DNA-PKcs but increased the expression level of TOX compared to those of the control group (Fig. 6b).

4. Discussion

An increasing number of natural products and their derivatives, including SAG, have rich structural diversity, promising therapeutic applications and possess antitumor activities [18–21]. SAG is a beneficial antitumor drug that induces cell death and inhibits tumorigenesis in a variety of cancers and synergistically enhances sensitivity to chemotherapy drugs [17]. Herein, we found that SAG inhibited the growth of GC cells *in vitro* and *in vivo* and induced cell apoptosis and cycle arrest but did not exert cytotoxicity on GES-1 cells.

Our previous study showed that SAG inhibited the proliferation and invasive potential of GC cells *in vitro via* the regulation of the DUSP4/ERK pathway [18]. However, the precise targets of SAG in GC remain unclear. In our study, TOX, identified as a target of SAG and GC by network pharmacology, showed low expression levels in GC tissues, and a low expression of TOX was an independent prognostic factor of poor survival in patients with GC. Moreover, TOX overexpression can significantly decrease cell proliferation, and SAG may act as a TOX activator, exerting its activity in GC. TOX, a nuclear and DNA-binding protein, is essential for the differentiation of thymocytes [22]. It is specifically expressed in T-cell malignancies, and its related members (TOX2/3/4) also cause dysregulation in malignant tumors [23–25]. The

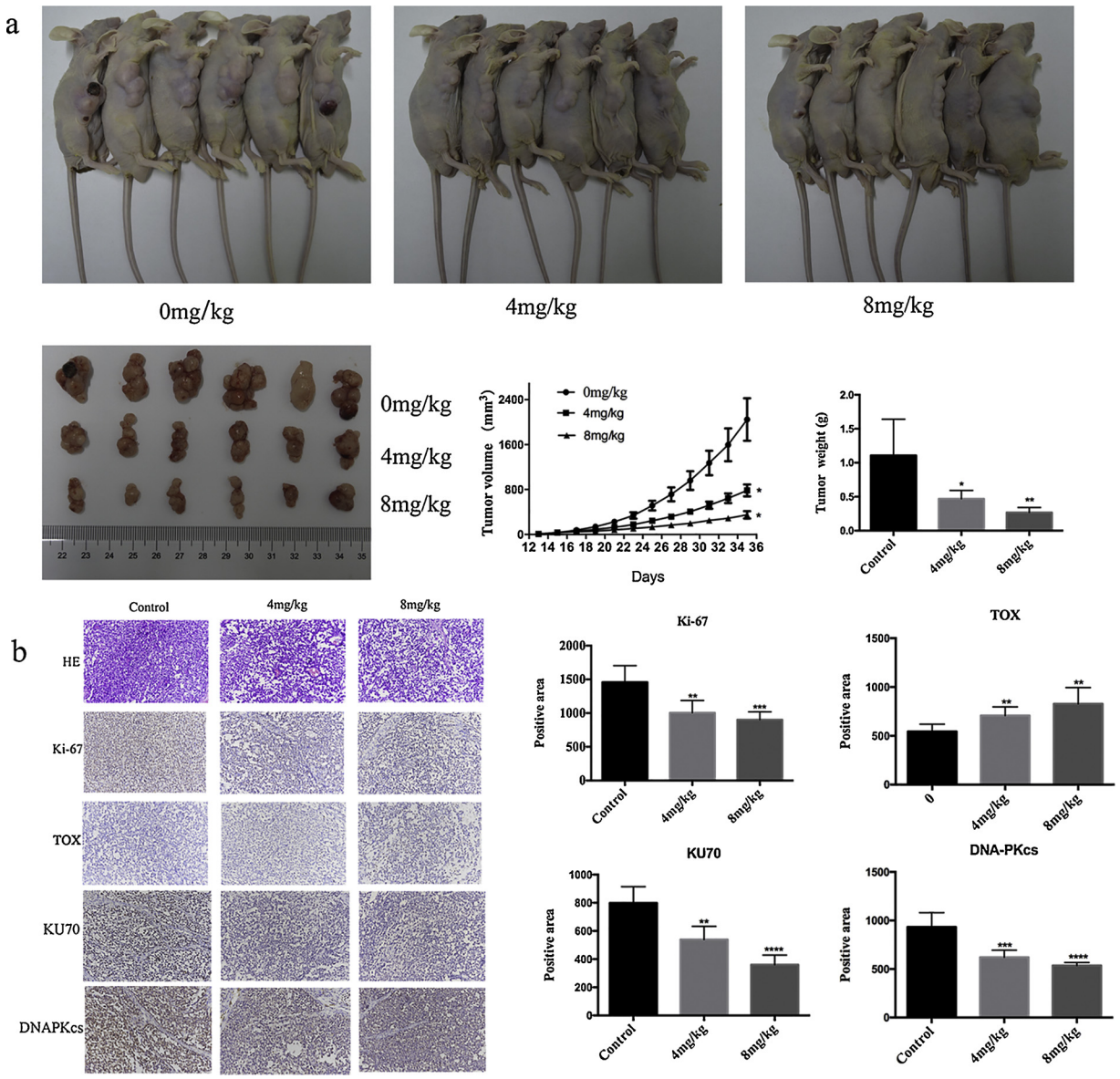

Fig. 6. SAG inhibited xenograft tumor growth. (a) Representative tumor sections from the control group and low- and high-dose SAG groups, and the comparison of the tumor volume and weight in these three groups. (b) H&E analysis of the tumor formation ability in the control and low- or high-dose SAG groups (×200), and IHC analysis of the expression levels of Ki-67, TOX, KU70, and DNA-PKcs in the tumor tissues from these three groups (×200). * $P < 0.05$, ** $P < 0.01$, *** $P < 0.001$, **** $P < 0.0001$.

low expression of TOX3 is associated with a poor prognosis in diffuse-type GC [26]. Therefore, TOX as the target of SAG may provide new strategies for GC.

NHEJ is a nonspecific repair mechanism and prone to errors. NHEJ repair is initiated by the recruitment of KU70/80 and DNA-PKcs to DNA damage [27,28] and leads to DNA translocations, inversions, and deletions in cancer [29]; its overactivation can regulate cell cycle arrest, apoptosis, chromosome recombination and genomic instability [30,31]. KU70/80 deficiency causes elevated genomic instability and T-cell malignancies [32,33]. However, the DNA-PKcs/KU70/80 axis has been confirmed to be upregulated in multiple cancers, including GC, and promotes their carcinogenesis [6,34–36]. Both DNA-PKcs and KU70/80 are overexpressed in GC tissues and promote malignant pathological processes [6], and the expression of KU70 was significantly higher in precancerous lesions and GC tissues compared with that in normal gastric mucosal tissues [37]. Another study confirmed the increased expression of DNA-PKcs in consecutive cases of GC by immunohistochemistry [38]. The latest study showed that TOX regulates DNA repair and genomic instability in T-cell acute lymphoblastic leukemia, binds directly to KU70/80, and inhibits NHEJ by suppressing recruitment of KU70/KU80 to sites of DNA damage [12]. In our study, in accordance with previous studies, we assessed the effects of SAG on the expression levels of DNA-PKcs/KU70/80 and found that SAG decreased the expression levels of DNA-PKcs and KU70/80 in GC cells, indicating that SAG might repress GC growth by regulating the TOX-mediated DNA-PKcs/KU70/80 axis.

5. Conclusion

In summary, we identified TOX as a target of SAG and GC and found that low expression of TOX was associated with poor survival in patients with GC; Moreover, SAG inhibited growth and induced cell apoptosis and cycle arrest in GC cells by regulating the TOX-mediated DNA-PKcs/KU70/KU80 axis. These findings might provide a therapeutic strategy for GC.

Declaration of Competing Interest

The authors declare that they have no competing interests.

Acknowledgments

This study was supported by grants from the National Natural Science Foundation of China (81573747 & 81873143).

Appendix A. Supplementary data

Supplementary material related to this article can be found, in the online version, at doi:https://doi.org/10.1016/j.prp.2019.152677.

References

[1] C. Allemani, H.K. Weir, H. Carreira, R. Harewood, D. Spika, X.S. Wang, F. Bannon, J.V. Ahn, C.J. Johnson, A. Bonaventure, R. Marcos-Gragera, C. Stiller, G.Silvae. Azevedo, W.Q. Chen, O.J. Ogunbiyi, B. Rachet, M.J. Soeberg, H. You, T. Matsuda, M. Bilska-Lasota, H. Storm, T.C. Tucker, M.P. Coleman, CONCORD Working Group, Global surveillance of cancer survival 1995-2009: analysis of individual data for 25,676,887 patients from 279 population-based registries in 67 countries (CONCORD-2), Lancet 385 (9972) (2015) 977–1010.

[2] F. Bray, J. Ferlay, I. Soerjomataram, R. Siegel, L.A. Torre, Ae. Jemal, Global cancer statistics 2018: GLOBOCAN estimates of incidence and mortality worldwide for 36 cancers in 185 countries, CA Cancer J. Clin. 68 (2018) 394–424.

[3] M. Shrivastav, C.A. Miller, L.P. Haro De, S.T. Durant, B.P. Chen, D.J. Chen, J.A. Nickoloff, DNA-PKcs and ATM co-regulate DNA double-strand break repair, DNA Repair (Amst). 8 (8) (2009) 920–929 2009.

[4] M.R. Lieber, J. Gu, H. Lu, N. Shimazaki, A.G. Tsai, Nonhomologous DNA end joining (NHEJ) and chromosomal translocations in humans, Subcell. Biochem. 50 (2010) 279–296.

[5] T. Abe, M. Ishiai, Y. Hosono, A. Yoshimura, S. Tada, N. Adachi, H. Koyama, M. Takata, S. Takeda, T. Enomoto, M. Seki, KU70/80, DNA-PKcs, and Artemis are essential for the rapid induction of apoptosis after massive DSB formation, Cell. Signal. 20 (11) (2008) 1978–1985.

[6] L. Wei, C. Xie, Z. Yang, J. Chen, N.H. Lu, Abnormal DNA-PKcs and Ku 70/80 expression may promote malignant pathological processes in gastric carcinoma, World J. Gastroenterol. 19 (40) (2013) 6894–6901.

[7] X. Yu, Z. Li, TOX gene: a novel target for human cancer gene therapy, Am. J. Cancer Res. 5 (12) (2015) 3516–3524.

[8] Y. Huang, M.W. Su, X. Jiang, Y. Zhou, Evidence of an oncogenic role of aberrant TOX activation in cutaneous T-cell lymphoma, Blood. 125 (9) (2015) 1435–1443.

[9] E. Braggio, E.R. McPhail, W. Macon, M.B. Lopes, D. Schiff, M. Law, S. Fink, D. Sprau, C. Ginannini, A. Dogan, R. Fonseca, B.P. O'Neill, Primary central nervous system lymphomas: a validation study of array-based comparative genomic hybridization in formalin-fixed paraffin-embedded tumor specimens, Clin. Cancer Res. 17 (13) (2011) 4245–4253.

[10] S. Safavi, M. Hansson, K. Karlsson, A. Biloglav, B. Johansson, K. Paulsson, Novel gene targets detected by genomic profiling in a consecutive series of 126 adults with acute lymphoblastic leukemia, Haematologica. 100 (1) (2015) 55–61.

[11] S. Morimura, M. Sugaya, H. Suga, et al., TOX expression in different subtypes of cutaneous lymphoma, Arch. Dermatol. Res. 306 (2014) 843–849.

[12] R. Lobbardi, J. Pinder, B. Marinez-Pastor, M. Theodorou, J.S. Blackburn, B.J. Abraham, Y. Namiki, M. Mansour, N.S. Abdelfattah, A. Molodtsov, G. Alexe, D. Toiber, M. Waard de, E. Jain, M. Boukhali, M. Lion, D. Bhere, K. Shah, A. Gutierrez, K. Stegmaier, L.B. Silverman, R.I. Sadreyev, J.M. Asara, M.A. Oettinger, W. Haas, A.T. Look, R.A. Young, R. Mostoslavsky, G. Dellaire, D.M. Langenau, Tox regulated growth, DNA repair, and genomic instability in T-cell acute lyphoblastic leukemia, Cancer Discov. 7 (11) (2017) 1336–1353.

[13] T. Chen, Q. Li, X. Zhang, R. Long, Y. Wu, J. Wu, X. Fu, Tox expression decreases with progression of colorectal cancers and is associated with $CD4^{+}$T-cell density and Fusobacterium nucleatum infection, Hum. Pathol. 79 (2018) 93–101.

[14] L.L. Laster, R.R. Lobene, New perspectives on sanguinaria clinicals: individual toothpaste and ora rinse testing, J. Can. Dent. Assoc. 56 (7 Suppl) (1990) 19–30.

[15] I.W. Achkar, F. Mraiche F, R.M. Mohammad, S. Uddin, Anticancer potential of sanguinarine for various human malignancies, Future Med. Chen. 9 (9) (2017) 933–950.

[16] A. Rahman, S. Pallichankandy, F. Thayyullathil, S. Galadari, Critical role of H_2O_2 in mediating sanguinarine-induced apoptosis in prostate cancer cells via facilitatine ceramide generation, ERK1/2 phosphorylation, and Par-4 cleavage, Free Radic. Biol. Med. 134 (2019) 527–544.

[17] S. Galadari, A. Rahman, S. Pallichankandy, F. Thayyullathil, Molecular targets and anticancer potential of sanguinarine-a benzophenanthridine alkaloid, Phytomedicine 34 (2017) 143–153.

[18] R. Zhang, G. Wang, P.F. Zhang, J. Zhang, Y.X. Huang, Y.M. Lu, W. Da, Q. Sun, J.S. Zhu, Sanguinarine inhibits growth and invasion of gastric cancer cells via regulation of the DUSP4/ERK pathway, J. Cell. Mol. Med. 21 (6) (2017) 1117–1127.

[19] J. Clardy, C. Walsh, Lessons from natural molecules, Nature 432 (7019) (2004) 829–837.

[20] B.B. Mishra, V.K. Tiwari, Natural products: an evolving role in future drug discovery, Eur. J. Med. Chem. 46 (10) (2011) 4769–4807.

[21] G. Wang, Y.X. Huang, R. Zhang, L.D. Hou, H. Liu, X.Y. Chen, J.S. Zhu, J. Zhang, Toosendanin suppresses oncogenic phenotypes of human gastric carcinoma SGC-7901 cells partly via miR-200a-mediatated downregulation of β-catenin pathway, Int. J. Oncol. 51 (5) (2017) 1563–1573.

[22] P. Aliahmad, A. Seksenyan, J. Kaye, The many roles of TOX in the immune system, Curr. Opin. Immunol. 24 (2) (2012) 173–177.

[23] M. Tessema, C.M. Yingling, M.J. Grimes, C.L. Thomas, Y. Liu, S. Leng, N. Joste, S.A. Belinsky, Differential epigenetic regulation of TOX subfamily high mobility group box genes in lung and breast cancers, PLoS One 7 (4) (2012) e34850.

[24] W. Chung, B. Kwabi-Addo, M. Ittmann, J. Jelinek, L. Shen, Y. Yu, J.P. Issa, Identification of novel tumor markers in prostate, colon and breast cancer by unbiased methylation profiling, PLoS One 3 (4) (2008) e2079.

[25] P. Lamesch, N. Li, S. Milstein, C. Fan, T. Hao, G. Szabo, Z. Hu, K. Venkatesan, G. Bethel, P. Martin, J. Rogers, S. Lawlor, A. Dricot, H. Borick, M.E. Cusick, J. Vandenhaute, I. Dunham, D.E. Hill, M. Vidal, hORFeome v3.1: a resource of human open reading frames representing over 10,000 human genes, Genomics 89 (3) (2007) 307–315.

[26] X. Zhang, H. Zhu, X. Wu, M. Wang, D. Gu, W. Gong, Z. Xu, Y. Tan, Y. Gong, J. Zhou, C. Tang, N. Tong, J. Chen, Z. Zhang, A genetic polymorphism in TOX3 is associated with survival of gastric cancer in a Chinese population, PLoS One 8 (9) (2013) e72186.

[27] P.A. Jeggo, Identification of genes involved in repair of DNA double- strand breaks in mammalian cells, Radiat. Res. 150 (5 Suppl) (1998) S80–S91.

[28] F. Dietlein, L. Thelen, H.C. Reinhardt, Cancer-specific defects in DNA repair pathways as targets for personalized therapeutic approaches, Trends Genet. 30 (8) (2014) 326–339.

[29] S.F. Bunting, A. Nussenzweig, End-joining, translocations and cancer, Nat. Rev. Cancer 31 (7) (2013) 443–454.

[30] J.R. Chapman, M.R. Taylor, S.J. Boulton SJ, Playing the end game: DNA double-strand break repair pathway choice, Mol. Cell 47 (2012) 497-451.

[31] M. Shrivastav, L.P. De Haro, J.A. Nickoloff, Regulation of DNA double-strand break repair pathway choice, Cell Res. 18 (2008) 134–147.

[32] Y. Gu, K.J. Seidl, G.A. Rathbun, C. Zhu, J.P. Manis, N. van der Stoep, L. Davidson, H.L. Cheng, J.M. Sekiguchi, K. Frank, P. Stanhope-Baker, M.S. Schlissel, D.B. Roth, F.W. Alt, Growth retardation and leaky SCID phenotype of Ku70-deficient mice, Immunity 7 (5) (1997) 653–665.

[33] A. Nussenzweig, C. Chen, V. da Costa Soares, M. Sanchez, K. Sokol, M.C. Nussenzweig, G.C. Li, Requirement for Ku80 in growth and immunoglobulin V (D)J recombination, Nature 382 (6591) (1996) 551–555.

[34] A.T. Alshareeda, O.H. Negm, N. Albarakati, A.R. Green, C. Nolan, R. Sultana, S. Madhusudan, A. Benhasouna, P. Tighe, I.O. Ellis, E.A. Rakha, Clinicopathological signi cance of KU70/KU80, a key DNA damage repair protein in breast cancer, Breast Cancer Res. Treat. 139 (2) (2013) 301–310.

[35] M.J. Kang, S.M. Jung, M.J. Kim, J.H. Bae, H.B. Kim, J.Y. Kim, S.J. Park, H.S. Song, D.W. Kim, C.D. Kang, S.H. Kim, DNA-dependent protein kinase is involved in heat shock protein-mediated accumulation of hypoxia-inducible factor-1alpha in hypoxic preconditioned HepG2 cells, FEBS J. 275 (23) (2008) 5969–5981.

[36] A. Gibaud, N. Vogt, O. Brison, M. Debatisse, B. Malfoy, Characterization at nucleotide resolution of the homogeneously staining region sites of insertion in two cancer cell lines, Nucleic Acids Res. 41 (2013) 8210–8219.

[37] H. Hu, Y. Zhang, M. Zou, S. Yang, X.Q. Liang, Expression of TRF1, TRF2, TIN2, TERT, KU70, and BRCA1 proteins is associated with telomere shortening and may contribute to multi- stage carcinogenesis of gastric cancer, J. Cancer Res. Clin. Oncol. 136 (2010) 1407–1414.

[38] H.S. Lee, G. Choe, K.U. Park, D.J. Park, H.K. Yang, B.L. Lee, W.H. Kim, Altered expression of DNA-dependent protein kinase catalytic subunit (DNA-PKcs) during gastric carcinogenesis and its clinical implications on gastric cancer, Int. J. Oncol. 31 (4) (2007) 859–866.